ELSEVIER

Chemical Engineering Journal 144 (2008) 188–196

Chemical Engineering Journal

www.elsevier.com/locate/cej

Adsorption of chromium(VI) from aqueous solution by activated carbon derived from olive bagasse and applicability of different adsorption models

Hakan Demiral *, İlknur Demiral, Fatma Tümsek, Belgin Karabacakoğlu

Department of Chemical Engineering, Faculty of Engineering and Architecture, Eskişehir Osmangazi University, Meşelik Campus, 26480 Eskişehir, Turkey

Received 23 February 2007; received in revised form 7 January 2008; accepted 15 January 2008

Abstract

In this study, activated carbon was prepared from olive bagasse by physical activation of steam. The pore properties including the BET surface area, pore volume, pore size distribution and average pore diameter were characterized. BET surface area of the activated carbon was determined as 718 m^2/g. The removal of Cr(VI) from aqueous solutions by adsorption has been studied. The effects of pH, contact time and temperature on adsorption of Cr(VI) were investigated. The maximum adsorption yield was obtained at the initial pH of 2. The adsorption kinetics shows that pseudo-second order rate expression fitted the adsorption kinetics. Equilibrium isotherms were measured experimentally. Results were analyzed by the Langmuir, Freundlich, Dubinin-Redushkevich, Temkin and Frumkin equations using linearized correlation coefficient at different temperatures. The characteristics parameters for each isotherm have been determined. Models and isotherm constants were evaluated depending on temperature. Langmuir equation was found to fit the equilibrium data for Cr(VI) adsorption.

Keywords: Chromium(VI); Adsorption; Adsorption isotherm; Activated carbon; Olive bagasse

1. Introduction

Metals and their derivatives are potential pollutants that can be particularly problematic due to their stability and mobility. Among them, chromium has become a serious health concern due to its release into the environment [1].

Chromium is one of the contaminants which exist in hexavalent and trivalent forms. Hexavalent form is more toxic than trivalent and requires more concern. Strong exposure to Cr(VI) causes cancer in the digestive tract and lungs and may cause epigastric pain, nausea, vomiting, severe diarrhea and hemorrhage [2]. It is therefore essential to remove Cr(VI) from wastewater before disposal.

Several industries like paint and pigment manufacturing, stainless steel production, corrosion control, leather tanning, chromium plating, wood preservation, fertilizers, textile, photography, etc., discharge effluent containing hexavalent chromium to surface water [3].

Conventional methods for removing dissolved heavy metal ions include chemical precipitation, chemical oxidation or reduction, filtration, ion exchange, electrochemical treatment, application of membrane technology. However, these processes have considerable disadvantages including incomplete metal removal, requirements for expensive equipment and monitoring system, high reagent and energy requirements or generation of toxic sludge or other waste products that require disposal [4,5].

Cr(VI) concentrations in industrial wastewater range from 0.5 mg/L to 270.000 mg/L. The tolerance limit for Cr(VI) for discharge into inland surface waters is 0.1 mg/L and in potable water is 0.05 mg/L [6].

Adsorption can be effective and versatile method for removing chromium particularly when combined with appropriate regeneration steps. This solves the problems of sludge disposal and renders the system more economically viable, especially if low cost adsorbents are used [7].

Many reports have already been published involving the low cost activated carbon adsorbents produced from cheaper and readily available materials [8–11]. Their high surface areas, microporous characters and surface chemical natures have made

* Corresponding author. Tel.: +90 222 2393750 3283.
E-mail address: hdemiral@ogu.edu.tr (H. Demiral).

1385-8947/$ – see front matter © 2008 Elsevier B.V. All rights reserved.
doi:10.1016/j.cej.2008.01.020

them potential adsorbents for the removal of heavy metals from industrial wastewater [7].

Studies on the removal of Cr(VI) by activated carbons produced from Tunçbilek lignite [7], coconut shell [12], *Casurina equisetifoli* leaves [13], rice husk [14], tyres and sawdust [15], etc., have all been reported in the literature.

Olive bagasse is the solid residue obtained from pressing the olives. In recent years olive bagasse production in Turkey has increased due to the increase of olive oil production. These residues are not used for the production of energy and other products in Turkey and thus it constitutes a source of environmental problems caused by its accumulation and disposal [16]. Reuse of these residues could solve pollution problems and recover valuable compounds such as activated carbon.

In the present study, activated carbon was produced from olive bagasse by steam activation. The resultant carbons were used to remove Cr(VI) from aqueous solutions and applicability of the various adsorption models for Cr(VI) adsorption were investigated.

2. Materials and methods

2.1. Materials

The olive waste composed of a crushed mixture of kernel and pulp, and a waste product of Turkish vegetable oil production using olives from the Marmara Region of Turkey.

A stock chromate solution of 1000 mg/L was prepared from potassium dichromate salt. The working solutions with different concentrations were prepared by appropriate dilutions of the stock solution. The initial pH of solutions was adjusted to the required value by using NaOH or HCl solutions.

2.2. Preparation of activated carbon

Carbonization was carried out in a horizontal tube furnace. Samples (20 g) were placed into the reactor and heated from room temperature to 500 °C at a constant heating rate of 10 °C/min under nitrogen flow, then held at 500 °C for 1 h. The samples were left to cool down after the carbonization.

Activation was carried out in a vertical tube furnace. The char obtained from carbonization was heated from room temperature to 850 °C under nitrogen flow. Once the activation temperature was reached, nitrogen flow was switched to steam. The duration of treatment at final temperature is 0.5 h. At the end of the activation period, the sample was cooled under nitrogen.

BET surface area, pore volumes, pore size distribution, micropore surface area and average pore diameter (APD) were determined by the N_2 adsorption at 77 K with Autosorb 1 C (Quantachrome).

2.3. Adsorption studies

2.3.1. The effect of pH

The effect of pH on Cr(VI) adsorption was investigated in the initial pH range of 2–10. The initial pH of the solution was adjusted by using 0.1N HCl or 0.1N NaOH. Dried activated carbon (0.1 g) was added to 50 mL of solution having 100 mg/L of Cr(VI) ions. After adsorption, the solutions were centrifuged and the concentrations of the solutions were determined.

2.3.2. Kinetic study

Pseudo-first order and pseudo-second order rate equations have been used for modeling the kinetics of Cr(VI) adsorption. The experiments were carried out at 35 and 45 °C to investigate the adsorption kinetics. For this purpose, 250 mL of the Cr(VI) solution (initial concentration = 500 mg/L) and 0.5 g activated carbon were agitated until reaching the adsorption equilibrium. Samples were pipetted out at different time intervals. The collected samples were analyzed using a UV spectrophotometer.

2.3.3. Adsorption isotherms

In the experiments, 0.1 g of activated carbon samples were mixed with 50 mL solutions of various Cr(VI) concentrations between 50 mg/L and 500 mg/L in the isothermal shaker for 10 h at 25 °C, 35 °C and 45 °C constant temperatures. After adsorption, the mixtures were centrifuged and the concentrations of Cr(VI) ions remaining unadsorbed were determined.

2.3.4. Analysis of Cr(VI)

The analysis of Cr(VI) was carried out colorimetrically with the 1,5-diphenyl carbazide method using a UV-120-01 model Shimadzu Spectrophotometer [17]. The amount of adsorbed Cr(VI) was calculated from the difference in their initial and final concentrations.

3. Results

3.1. Physical properties

Identifying the pore structure of adsorbent, which is commonly determined by the adsorption of inert gases, is an essential procedure before designing the adsorption process [18]. Fig. 1 shows the adsorption–desorption isotherm of N_2 at 77 K. Adsorption data were obtained over the relative pressure, P/P_0, range from 10^{-7} to 1. Surface area of the activated carbon was calculated by BET (Brunauer–Emmett–Teller) equation within the 0.01–0.15 relative pressure range. Micropore volume, micropore area and external surface area were calculated

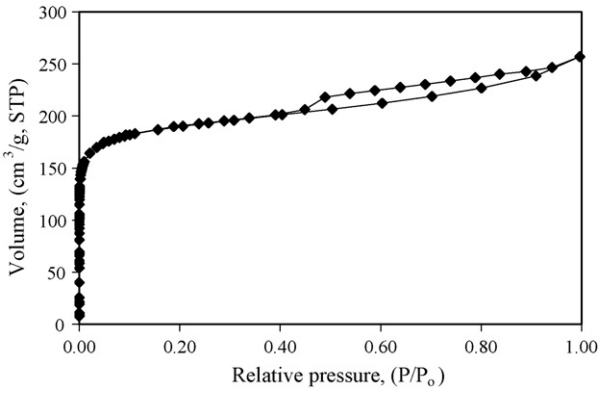

Fig. 1. Adsorption–desorption isotherm of the activated carbon.

Table 1
Physical properties of the activated carbon

S_{BET} (m^2/g)	718
S_{micro} (m^2/g)	585
S_{ext} (m^2/g)	133
V_{micro} (cm^3/g)	0.3149
V_{meso} (cm^3/g)	0.055
V_T (cm^3/g)	0.3699
APD (nm)	2.2

by using the *t*-plot method. Pore size distribution was obtained applying the Density Functional Theory (DFT) method to the adsorption isotherm. The total pore volume was determined from the amount of N_2 adsorbed at a relative pressure close to unity (~0.99) by assuming that the pores are then filled with liquid adsorbate (N_2). All calculations were performed by using the software supplied by Autosorb 1C. Mesopore volume was calculated by subtracting the micropore volume from total pore volume.

One of the methods for estimating the type of pores present in a solid is by analyzing the adsorption isotherm curve. The graph of the adsorption isotherm in Fig. 1 is a Type I isotherm and this indicates that the activated carbon is microporous. Initial step region of the isotherm is abruptly followed by a plateau indicating that the adsorption has virtually stopped because multilayer of adsorbate cannot be formed due to close proximity of the pore wall.

The physical properties of activated carbon determined from the adsorption isotherm were given in Table 1. As seen in Table 1, the micropore volume (V_{micro}) occupies the 85% of the total pore volume.

Pore size distribution of activated carbon which was calculated by using DFT method was given in Fig. 2. Activated carbon exhibits two peaks around 4–20 Å (0.4–2 nm) and 30–41 Å (3–4.1 nm). The structures of the porous activated carbons are classified into three groups as micropore (<2 nm), mesopore (2–50 nm) and macropore (>50 nm) according to the International Union of Pure and Applied Chemistry (IUPAC). The activated carbon produced from olive bagasse in this study contains both micropores and mesopores but the micropore volume is larger than the mesopore volume.

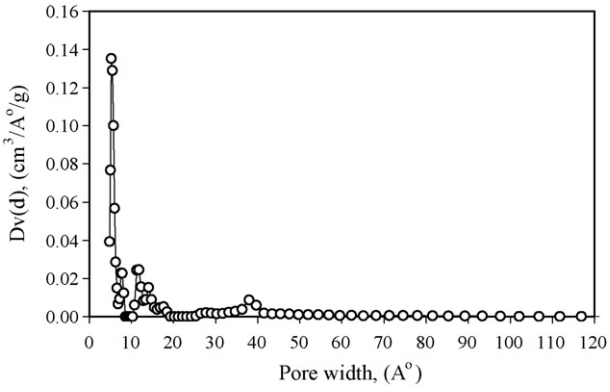

Fig. 2. Pore size distribution of activated carbon.

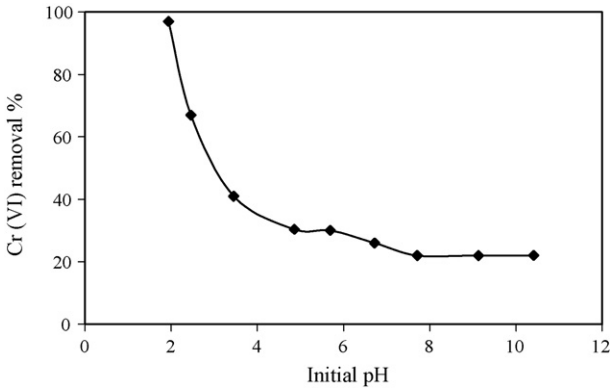

Fig. 3. The effect of initial pH on adsorption of Cr(VI) (initial Cr(VI) conc., 100 mg/L; volume of Cr(VI) solution, 50 mL; amount of activated carbon, 0.1 g; temperature, 25 °C).

3.2. Adsorption studies

3.2.1. Effect of initial pH

The solution pH is one of the parameters having considerable influence on the adsorption of metal ions, because the surface charge density of the adsorbent and the metallic species depend on the pH [19]. The effect of the pH on the adsorption of Cr(VI) is seen in Fig. 3. The adsorption increases from 11.2 mg/g (22% removal) to 48.5 mg/g (97% removal) because of the decrease of pH from 10.4 to 2. This indicates that the Cr(VI) adsorption capacity of the adsorbent is dependent upon pH.

Hexavalent chromium exists in different forms in aqueous solution such as $HCrO_4^-$, $Cr_2O_7^{2-}$, CrO_4^- and the stability of these forms is mainly dependent on the pH of the system [20]. The behavior for better adsorption at low pH by activated carbon may be attributed to the large number of H^+ ions present at low pH values which in turn neutralize the negatively charged adsorbent surface, thereby reducing hindrance to the diffusion of chromate ions [21]. It is well known that the dominant form of Cr(VI) between pH 1.0 and 4.0 is $HCrO_4^-$ [20]. So that $HCrO_4^-$ is adsorbed preferentially on carbon. The decrease in removal at higher pH may be due to abundance of OH^- ions causing increased hindrance to diffusion of dichromate ions. Increasing the pH will shift the concentration of $HCrO_4^-$ to other forms. Similar observations have also been reported by other investigators [21,22]. Because of the solution at a pH value about 2 is an optimal condition for the adsorption of Cr(VI), following studies were carried out at initial pH of 2. It was reported that Cr(VI) could be reduced to Cr(III) in the presence of activated carbon under highly acidic conditions (pH < 2). The Cr(III) ions could precipitate as hydroxide at high pH values in low Cr(III) concentrations [4,6]. On the other hand, the pH value increased from 2 to 4 at the end of the experiments in this study and precipitation of Cr(III) ions is not possible at such a low pH and low Cr(III) concentration values.

3.2.2. Effect of time

Fig. 4 shows the effect of contact time on the batch adsorption of 500 ppm Cr(VI) at 35 and 45 °C by activated carbon. The amount of Cr(VI) adsorbed increased with increase in agitation

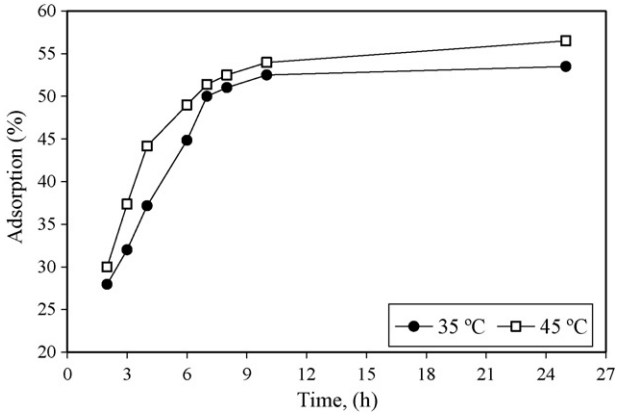

Fig. 4. The effect of time on Cr(VI) adsorption at different temperatures (initial Cr(VI) conc., 500 mg/L; volume of Cr(VI) solution, 250 mL; amount of activated carbon, 0.5 g; pH, 2).

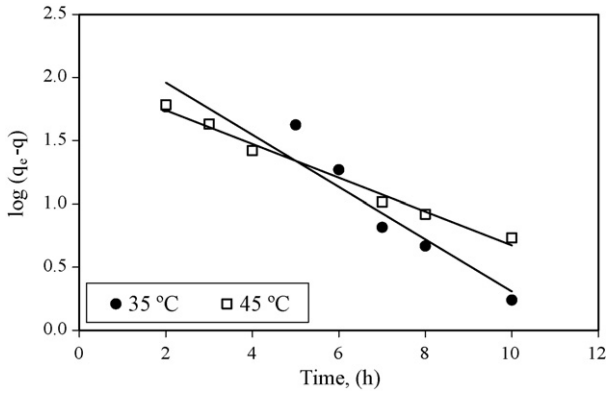

Fig. 5. Pseudo-first order kinetics plots for the removal of Cr(VI) (initial Cr(VI) conc., 500 mg/L; volume of Cr(VI) solution, 250 mL; amount of activated carbon, 0.5 g; pH, 2).

time. Equilibrium time for Cr(VI) removal was 10 h. The percentage of Cr(VI) removed at equilibrium increased from 52% to 54% as the temperature of solution increased from 35 °C to 45 °C. No change in the uptake capacity was observed with further increase the contact time up to 24 h. It is clear that the removal of Cr(VI) depends on the temperature of the solution.

3.2.3. Kinetics of adsorption

The study of adsorption kinetics is significant as it provides valuable insights into the reaction pathways and the mechanism of the reactions. Any adsorption process is normally controlled by the three diffusion steps: (i) transport of the solute from bulk solution to the film surrounding the adsorbent, (ii) from the film to the adsorbent surface, (iii) from the surface to the internal sites followed by binding of the metal ions to the active sites. The slowest steps determine the overall rate of the adsorption process and usually it is thought that the step (ii) leads to surface adsorption and the step (iii) leads to intra-particle adsorption [19].

Several kinetic models are used to explain the mechanism of the adsorption processes. A simple pseudo-first order equation is given by Lagergren equation [19]:

$$\log(q_e - q) = \log q_e - \frac{k_i t}{2.303} \quad (1)$$

where q_e and q are the amounts of Cr(VI) adsorbed (mg/g) at equilibrium time and any time t, respectively, and k_1 is the rate constant of adsorption (h^{-1}). Plot of $\log(q_e - q)$ versus t gives a straight line for first order adsorption kinetics which allow computation of the rate constant k_1 (Fig. 5). The calculated linear regression correlation coefficients (R^2) were relatively small (0.9115 and 0.9769 for 35 °C and 45 °C, respectively) and the experimental q_e values did not agree with the calculated values obtained from the linear plots.

On the other hand, the pseudo-second order equation based on equilibrium adsorption is expressed as [19]

$$\frac{t}{q} = \frac{1}{k_2 q_e^2} + \frac{t}{q_e} \quad (2)$$

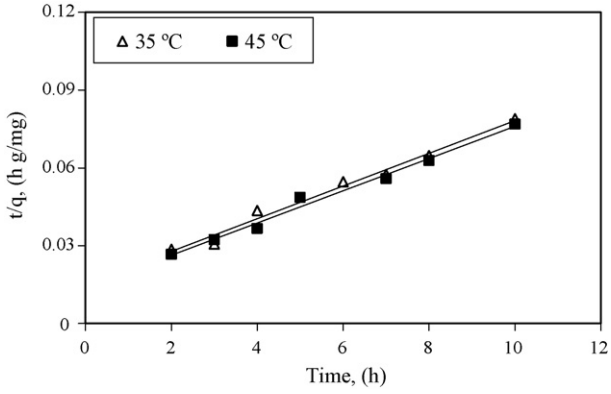

Fig. 6. Pseudo-second order kinetics plots for the removal of Cr(VI) (initial Cr(VI) conc., 500 mg/L; volume of Cr(VI) solution, 250 mL; amount of activated carbon, 0.5 g; pH, 2).

where k_2 is the pseudo-second order rate constant (g/mg h), q_e and q represent the amount of Cr(VI) adsorbed (mg/g) at equilibrium and at any time. The equilibrium adsorption capacity (q_e), and the second order constants (k_2) can be determined experimentally from the slope and intercept of plot t/q versus t (Fig. 6). The calculated q_e, k_2 and the corresponding linear regression correlation coefficient values are summarized in Table 2. R^2 values are greater than 0.985 for all temperature. As seen from Table 2, the values of q_e calculated from pseudo-second order kinetics almost agreed well with the experimental values of q_e. These results indicate that the adsorption of Cr(VI) on the prepared activated carbon follows pseudo-second order kinetics. Similar results have been observed for Cr(VI) adsorption [15,19].

Table 2
Pseudo-second order constants for the removal of Cr(VI) by activated carbon

T (°C)	k_2 (g/mg h)	$q_{e,exp}$ (mg/g)	$q_{e,cal}$ (mg/g)	R^2
35	0.00316	126.67	139.21	0.985
45	0.00314	136.63	146.29	0.991

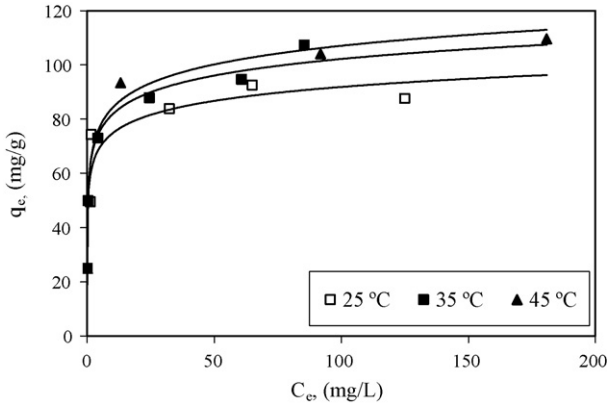

Fig. 7. Adsorption isotherms for Cr(VI)-activated carbon system at different temperatures (Cr(VI) conc., 50–500 mg/L; volume of Cr(VI) solution, 50 mL; amount of activated carbon, 0.1 g; pH, 2; contact time, 10 h).

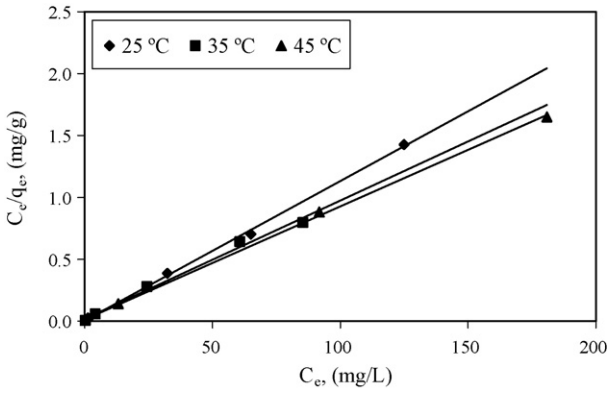

Fig. 8. Langmuir plots for adsorption of Cr(VI) at different temperatures. (Cr(VI) conc., 50–500 mg/L; volume of Cr(VI) solution, 50 mL; amount of activated carbon, 0.1 g; pH, 2; contact time, 10 h).

3.2.4. Adsorption isotherms

Fig. 7 shows the equilibrium isotherms for adsorption of chromium onto activated carbon at different temperatures. The isotherm rises in the initial stages with higher slope at low C_e and q_e values. This indicates that, initially, there are numerous readily accessible sites. At higher C_e values, a plateau occurs. This confirms the monolayer coverage of Cr(VI) onto activated carbon particles. Temperature has a pronounced effect on the adsorption capacity of adsorbents. The adsorptivity of Cr(VI) increases with the increase in temperature. This suggests that the adsorption process in nature is endothermic when temperature increased from 25 °C to 45 °C.

The increase in the adsorption capacity with increasing temperature may be due to the increase in the mobility and diffusion of adsorbate species. An increasing number of molecules may also acquire sufficient energy to undergo an interaction with active sites at the surface [23]. Since diffusion is an endothermic process, it would be expected that an increased solution temperature would result in the enlargement of pore size due to activated diffusion causing the micropores to widen and deepen (pore burrowing) and create more surface for adsorption [7,24,25].

The Langmuir, Freundlich, Dubinin–Radushkevich, Temkin and Frumkin adsorption isotherm models at different temperatures were examined to describe the adsorption equilibrium.

According to Langmuir model, adsorption occurs uniformly on the active sites of the adsorbent, and once an adsorbate occupies a site, no further adsorption can take place at this site [26]. Thus, the Langmuir model is given by the following equation:

$$\frac{C_e}{q_e} = \frac{1}{Q_0 b} + \frac{C_e}{Q_0} \tag{3}$$

where Q_0 and b, the Langmuir constants, are the saturated monolayer adsorption capacity (mg/g) and the adsorption equilibrium constant (L/mg), respectively. C_e is the equilibrium solution concentration (mg/L), q_e is the amount of Cr(VI) adsorbed at the equilibrium (mg/g). A plot of (C_e/q_e) versus C_e should yield a straight line if the Langmuir equation is obeyed by the adsorption equilibrium. The slope and the intercept of this line then give the values of Q_0 and b. Langmuir plots of for adsorption of Cr(VI) on activated carbon at different temperatures were given in Fig. 8.

A further analysis of the Langmuir equation can be made on the basis of a dimensionless equilibrium parameter, R_L, also known as the separation factor, given by [26]

$$R_L = \frac{1}{1 + bC_0} \tag{4}$$

where b is the Langmuir constant and C_0 is the initial Cr(VI) concentration (mg/L). If the average of the R_L values for each of the different initial concentrations used is between 0 and 1, it indicates favorable adsorption. The adsorption coefficients and the correlation coefficients were given in Table 3.

The Langmuir plots have good linearity ($R > 0.99$). The Langmuir monolayer adsorption capacity (Q_0) increased from 88.59 mg/g to 109.89 mg/g, as the temperature increased from 25 °C to 45 °C. In all of the temperatures, the values of R_L were calculated between 0 and 1, indicating the favorable adsorption of Cr(VI) on activated carbon derived from olive bagasse.

The Freundlich isotherm is an empirical model that is based on adsorption on heterogonous surface [26] and is given by the following equation:

$$\log q_e = \log k + \left(\frac{1}{n}\right) \log C_e \tag{5}$$

where q_e is the adsorption capacity (mg/g), C_e is the equilibrium concentration of the Cr(VI) solution (mg/L), k and n are Freundlich constants, which represent adsorption capacity and adsorption intensity, respectively. The Freundlich constants were determined from the slope and intercept of a plot of $\log q_e$ versus $\log C_e$ (Fig. 9) and were reported in Table 3.

The values of k and n changed with the rise in temperature. The magnitude of the n shows an indication of the favorability of adsorption. Values of n larger than 1 show the favorable nature of adsorption [27,28]. The values of n (Table 3) suggest that Cr(VI)

Table 3
Constant parameters and correlation coefficients calculated for different adsorption models at different temperatures for Cr(VI) adsorption

Isotherms	Solution temperature (K)	Constants			
		Q_0 (mg/g)	b (L/mg)	R_L	R^2
Langmuir	298	88.59	0.354	0.0021	0.998
	308	104.16	0.539	0.0122	0.992
	318	109.89	0.714	0.0092	0.999

Isotherms	Solution temperature (K)	Constants		
		k (mg/g)	n (L/mg)	R^2
Freundlich	298	62.90	7.063	0.895
	308	65.02	6.369	0.983
	318	67.05	6.098	0.914

Isotherms	Solution temperature (K)	Constants			
		q_m ($\times 10^3$ mol/g)	B ($\times 10^3$ mol^2/kJ^2)	E (kJ/mol)	R^2
D–R	298	2.364	1.122	21.11	0.935
	308	2.657	1.195	20.45	0.996
	318	2.959	1.386	18.99	0.952

Isotherms	Solution Temperature (K)	Constants		
		B_1 (mg/g)	A (L/mg)	R^2
Temkin	298	7.427	2348.11	0.908
	308	8.865	1015.75	0.985
	318	9.942	474.88	0.980

Isotherms	Solution temperature (K)	Constants			
		a	$\ln k$	$-\Delta G$ (kJ/mol)	R^2
Frumkin	298	−6.936	15.468	33.37	0.851
	308	−6.526	15.350	39.32	0.977
	318	−6.648	14.474	38.28	0.955

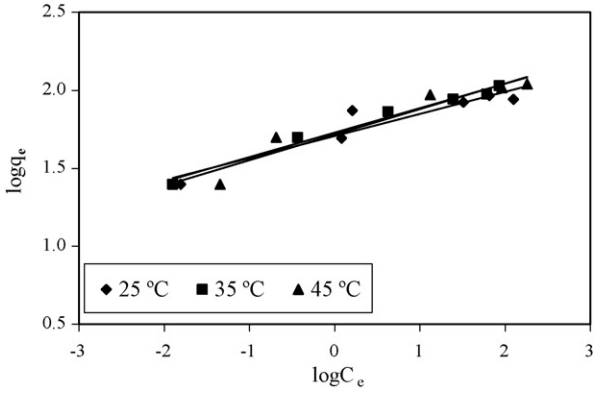

Fig. 9. Freundlich plots for adsorption of Cr(VI) at different temperatures (Cr(VI) conc., 50–500 mg/L; volume of Cr(VI) solution, 50 mL; amount of activated carbon, 0.1 g; pH, 2; contact time, 10 h).

are favorably adsorbed by activated carbon prepared from olive bagasse.

Another equation used in the analysis of isotherms was proposed by Dubinin–Radushkevich (D–R) [29,30]

$$q_e = q_s \exp(-B\varepsilon^2) \quad (6)$$

where q_s is the D–R constant and ε can be correlated as

$$\varepsilon = RT \ln\left[1 + \frac{1}{C_e}\right] \quad (7)$$

where R is the gas constant (8.314 J/mol K) and T is the absolute temperature. The isotherm constants of q_s and B (Table 3) are obtained from the intercept and the slope of the plot of $\ln q_e$ versus ε^2, respectively (Fig. 10). The constant B gives the mean free energy, E, of sorption per molecule of the sorbate when it is transferred to the surface of the solid from infinity in the solution and can be computed by using the following relationship [29,30]

$$E = \left[\frac{1}{\sqrt{2B}}\right] \quad (8)$$

The magnitude of E is useful for estimating the type of adsorption process. It was found to be in the range of 18.99–21.11 kJ/mol, which is bigger then the energy range of adsorption reactions, 8–16 kJ/mol [26]. The type of adsorption of Cr(VI) on the prepared activated carbon was defined as chemical adsorption.

Temkin and Pyzhev considered the effects of indirect adsorbate/adsorbate interactions on adsorption isotherms. The heat of adsorption of all the molecules in the layer would decrease lin-

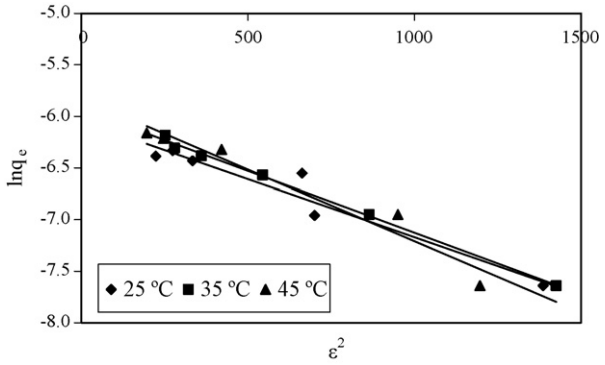

Fig. 10. D–R plots for adsorption of Cr(VI) at different temperatures (Cr(VI) conc., 50–500 mg/L; volume of Cr(VI) solution, 50 mL; amount of activated carbon, 0.1 g; pH, 2; contact time, 10 h).

early with coverage due to adsorbate/adsorbate interactions. The Temkin isotherm has been used in the form as follows [29,30]

$$q_e = \frac{RT}{b} \ln AC_e \tag{9}$$

Eq. (9) can be linearized as

$$q_e = B_1 \ln A + B_1 \ln C_e \tag{10}$$

where $B_1 = RT/b$, T is the absolute temperature (K), R is the gas constant (8.314 J/mol K), A is the equilibrium binding constant (L/mg) and B_1 is related to the heat of adsorption. A plot of q_e versus $\ln C_e$ (Fig. 11) enables the determination of the isotherm constants of B_1 and A from the slope and the intercept, respectively. The Temkin constants with the R^2 values are shown in Table 3. The Temkin isotherm constant in Table 3 shows that the heat of adsorption (B_1) increases with increase in temperature, indicating endothermic adsorption.

Frumkin equation which takes into account interaction between the adsorbed species can be expressed as [31,32]

$$\frac{\theta}{1-\theta} e^{-2a\theta} = k\, C_e \tag{11}$$

where θ is the fractional occupation ($\theta = q_e/q_m$; q_e is the adsorption capacity in equilibrium (mg/g), q_m is the theoretical monolayer saturation capacity (mg/g)). Eq (11) can be linearized as

$$\ln\left[\left(\frac{\theta}{1-\theta}\right)\frac{1}{C_e}\right] = \ln k + 2a\theta \tag{12}$$

The parameters a and k are obtained from the slope and intercept of the plot $\ln[(\theta/1-\theta)1/C_e]$ versus θ. The constant k is related to adsorption equilibrium

$$\ln k = \frac{-\Delta G}{RT} \tag{13}$$

Frumkin isotherm was given in Fig. 12 and isotherm constant were summarized in Table 3. The Frumkin equation has been specifically developed to take lateral interactions at the surface into account. The term $e^{-2a\theta}$ in Eq. (11) reflects the extent of lateral interactions; if $a > 0$ indicates attraction, while $a < 0$ means repulsion [32].

The correlation coefficients values of different isotherm models are listed in Table 3. The Langmuir isotherm model has higher regression coefficient ($R^2 > 0.99$) when compared to the other models. The increase in Langmuir constant b with temperature confirms the endothermic nature of the adsorption.

3.2.5. Thermodynamic parameters

Thermodynamic parameters such as Gibbs free energy (ΔG°), enthalpy (ΔH°) and entropy (ΔS°) were calculated using the following equations [1,26].

$$K_c = \frac{q_e}{C_e} \tag{14}$$

$$\Delta G^\circ = -RT \ln K_c \tag{15}$$

$$\ln K_c = \frac{\Delta S^\circ}{R} - \frac{\Delta H^\circ}{RT} \tag{16}$$

where K_c is the equilibrium constant, q_e is the solid phase concentration at equilibrium (mg/L) and C_e is the equilibrium concentration in solution (mg/L). ΔH° and ΔS° were obtained from the slope and intercept of linear Van't Hoff plots of $\ln K_c$ versus $1/T$. Table 4 shows the calculated values of the thermodynamic parameters for the adsorption of Cr(VI) on activated carbon.

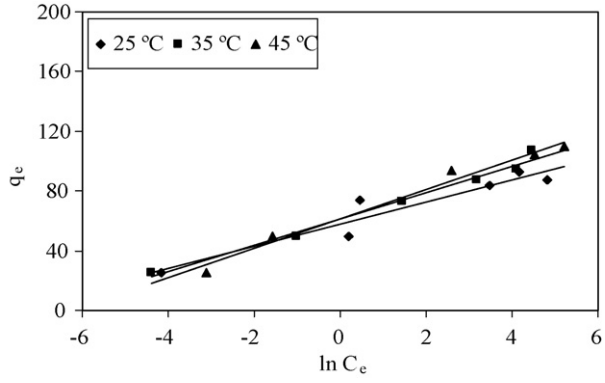

Fig. 11. Temkin plots for adsorption of Cr(VI) at different temperatures (Cr(VI) conc., 50–500 mg/L; volume of Cr(VI) solution, 50 mL; amount of activated carbon, 0.1 g; pH, 2; contact time, 10 h).

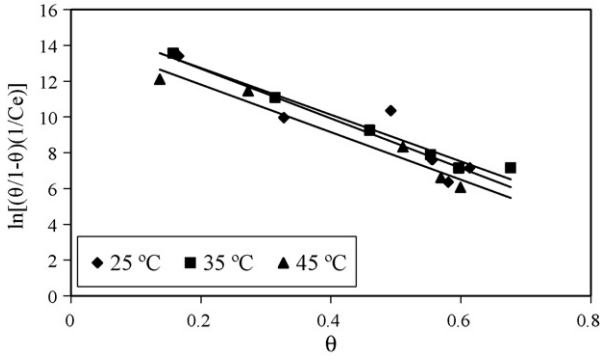

Fig. 12. Frumkin plots for adsorption of Cr(VI) at different temperatures (Cr(VI) conc., 50–500 mg/L; volume of Cr(VI) solution, 50 mL; amount of activated carbon, 0.1 g; pH, 2; contact time, 10 h).

Table 4
Thermodynamic parameters for the adsorption of Cr(VI) on activated carbon

T (K)	ΔG° (kJ/mol)	ΔH° (kJ/mol)	ΔS° (kJ/mol K)
298	−4.07		
308	−5.05	39.45	0.145
318	−7.02		

The negative values of ΔG° at various temperatures indicate the spontaneous nature of the adsorption process. The increase in ΔG° with increasing temperature shows that the adsorption is more favorable at high temperature. The positive value of ΔS° indicates that there is an increase in the randomness in the system solid/solution interface during the adsorption process. The positive value of ΔH° indicates that the adsorption is endothermic. Similar results have been reported for the Cr(VI) adsorption [1,26].

4. Conclusions

In this study, olive bagasse was converted into activated carbon by steam activation and used for the removal of Cr(VI) from aqueous solutions. The adsorption was found to be strongly dependent on pH. The uptake of Cr(VI) by activated carbon was maximal at pH 2. The kinetic studies showed that pseudo-second order rate equation was able to provide a realistic description of adsorption kinetics of Cr(VI). An increase in the adsorption capacity with the increase of temperature reveals that the adsorption is chemical in nature and the process in endothermic, which is confirmed by the thermodynamical parameters. Langmuir, Freundlich, Dubinin–Radushkevich (D–R), Temkin and Frumkin equations were used to describe the adsorption of Cr(VI) onto prepared activated carbon. Langmuir model has better correlation coefficient than the other models in the concentration studied at all temperatures. Thus, the results show that the activated carbon from olive bagasse can be effectively applied for the removal of Cr(VI) from wastewater.

Acknowledgement

The authors acknowledge the Scientific Research Fund of Eskisehir Osmangazi University for financial support (Project No: 2005/15007).

References

[1] J. Romero-Gonzalez, J.R. Peralta-Videa, E. Rodriguez, S.L. Ramirez, J.L. Gardea-Torresdey, Determination of thermodynamic parameters of Cr(VI) adsorption from aqueous solution onto *Agave lechuguilla* biomass, J. Chem. Thermodyn. 37 (2005) 343–347.
[2] K. Mohanty, M. Jha, B.C. Meikap, M.N. Biswas, Removal of chromium (VI) from dilute aqueous solutions by activated carbon developed from *Terminalia arjuna* nuts activated with zinc chloride, Chem. Eng. Sci. 60 (2005) 3049–3059.
[3] F. Gode, E. Pehlivan, Removal of Cr(VI) from aqueous solution by two Lewatit-anion exchange resins, J. Hazard. Mater. 119 (2005) 175–182.
[4] A. Baran, E. Bıçak, Ş. Hamarat-Baysal, S. Önal, Comparative studies on the adsorption of Cr(VI) ions on to various sorbents, Bioresour. Technol. 98 (2006) 661–665.
[5] Z. Aksu, F. Gönen, Z. Demircan, Biosorption of chromium(VI) ions by Mowital®B30H resin immobilized activated sludge in a packed bed: comparison with granular activated carbon, Process. Biochem. 38 (2002) 175–186.
[6] M. Kobya, Removal of Cr(VI) from aqueous solutions by adsorption onto hazelnut shell activated carbon: kinetic and equilibrium studies, Bioresour. Technol. 91 (2004) 317–321.
[7] R. Yavuz, I. Orbak, N. Karatepe, Factors affecting the adsorption of chromium (VI) on activated carbon, J. Environ. Sci. Health: A 41 (2006) 1967–1980.
[8] F.C. Wu, R.L. Tseng, R.S. Juang, Preparation of highly microporous carbons from fir wood by KOH activation for adsorption of dyes and phenols from water, Sep. Purif. Technol. 47 (2005) 10–19.
[9] R. Arriagada, R. Garcia, M. Molina-Sabio, F. Rodríguez-Reinoso, Effect of steam activation on the porosity and chemical nature of activated carbons from Eucalyptus globulus and peach stones, Micropor. Mater. 8 (1997) 123–130.
[10] J.A. Macia-Agullo, B.C. Moore, D. Cazorla-Amoros, A. Linares-Solano, Activation of coal tar pitch carbon fibres: physical activation vs. chemical activation, Carbon 42 (2004) 1367–1370.
[11] C.F. Chang, C.Y. Chang, W.T. Tsai, Effects of burn-off and activation temperature on preparation of activated carbon from corn cob agrowaste by CO_2 and steam, J. Colloid Interface Sci. 232 (2000) 45–49.
[12] S.J. Park, Y.S. Jang, Pore structure and surface properties of chemically modified activated carbons for adsorption mechanism and rate of Cr(VI), J. Colloid Interface Sci. 249 (2002) 458–463.
[13] K. Ranganathan, Chromium removal by activated carbons prepared from *Casurina equisetifolia* leaves, Bioresour. Technol. 73 (2000) 99–103.
[14] N.R. Bishnoi, M. Bajaj, N. Sharma, A. Gupta, Adsorption of Cr(VI) on activated rice husk carbon and activated alumina, Bioresour. Technol. 91 (2004) 305–307.
[15] N.K. Hamadi, X.D. Chen, M.M. Farid, M.G.Q. Lu, Adsorption kinetics for the removal of chromium(VI) from aqueous solution by adsorbents derived from used tyres and sawdust, Chem. Eng. J. 84 (2001) 95–105.
[16] S. Şensöz, İ. Demiral, H.F. Gerçel, Olive bagasse (*Olea europea* L.) pyrolysis, Bioresour. Technol. 97 (2006) 429–436.
[17] Standart Methods for the Examination of Water and Wastewater, 16th ed., APHA, AWWA, WPCE, Washington, DC, 1985, pp. 201–204.
[18] R.L. Tseng, S.K. Tseng, F.C. Wu, Preparation of high surface area carbons from corncob with KOH etching plus CO_2 gasification for the adsorption of dyes and phenols from water, Colloid Surf. A 279 (2006) 69–78.
[19] A. Sharma, K.G. Bhattacharyya, Adsorption of chromium(VI) on *Azadirachta Indica* (Neem) leaf powder, Adsorption 10 (2004) 327–338.
[20] V.K. Singh, P.N. Tiwari, Removal and recovery of chromium(VI) from industrial waste water, J. Chem. Technol. Biotechnol. 69 (1997) 376–382.
[21] M. Rao, A.V. Parwate, A.G. Bhole, Removal of Cr^{6+} and Ni^{2+} from aqueous solution using bagasse and fly ash, Waste Manage. 22 (2002) 821–830.
[22] H. Ucun, Y.K. Bayhan, Y. Kaya, A. Cakici, O.F. Algur, Biosorption of chromium(VI) from aqueous solution by cone biomass of *Pinus sylvestris*, Bioresour. Technol. 85 (2002) 155–158.
[23] E. Malkoç, Y. Nuhoğlu, Potential of tea factory waste for chromium(VI) removal from aqueous solutions: Thermodynamic and kinetic studies, Sep. Purif. Technol. 54 (2007) 291–298.
[24] D. Mohan, K.P. Singh, V.K. Singh, Trivalent chromium removal from wastewater using low cost activated carbon derived from agricultural waste material and activated carbon fabric cloth, J. Hazard. Mater. 135 (2006) 280–295.
[25] A. Agrawal, K.K. Sahu, B.D. Pandey, Systematic studies on adsorption of lead on sea nodule residues, J. Colloid Interface Sci. 281 (2005) 291–298.
[26] E. Oguz, Adsorption characteristics and the kinetics of the Cr(VI) on the *Thuja oriantalis*, Colloid Surf. 252 (2005) 121–128.
[27] N. Daneshvar, D. Salari, S. Aber, Chromium adsorption and Cr(VI) reduction to trivalent chromium in aqueous solutions by soya cake, J. Hazard. Mater. 94 (2002) 49–61.
[28] P.K. Malik, Dye removal from wastewater using activated carbon developed from sawdust: adsorption equilibrium and kinetics, J. Hazard. Mater. 113 (2004) 81–88.

[29] V.S. Mane, I.D. Mall, V.C. Srivastava, Use of bagasse fly ash as an adsorbent for the removal of brilliant green dye from aqueous solution, Dyes Pigment 73 (2007) 269–278.

[30] I.A.W. Tan, B.H. Hameed, A.L. Ahmad, Equilibrium and kinetic studies on basic dye adsorption by oil palm fibre activated carbon, Chem. Eng. J. 127 (2007) 111–119.

[31] C.A. Başar, Applicability of the various adsorption models of three dyes adsorption onto activated carbon prepared waste apricot, J. Hazard. Mater. 135 (2006) 232–241.

[32] N.K. Lazaridis, D.N. Bakoyannakis, E.A. Deliyanni, Chromium(VI) sorptive removal from aqueous solutions by nanocrystalline akaganeite, Chemosphere 58 (2005) 65–73.